Journal of Materials Chemistry A

Accepted Manuscript

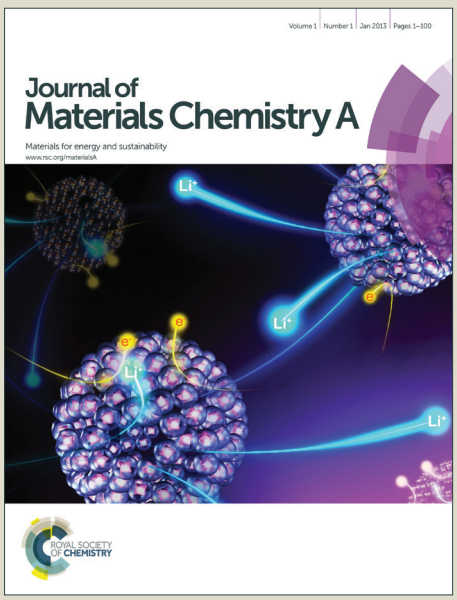

ROYAL SOCIETY OF CHEMISTRY

www.rsc.org/materialsA

Journal of Materials Chemistry A RSCPublishing

PAPER

Preparation of mesoporous Cu-Mn/TiO_2 composites for degradation of Acid Red 1

Cite this: DOI: 10.1039/x0xx00000x

Hongyang Min,‡[a] Xianqiang Ran,‡[a] Jianwei Fan,*[ab] Yu Sun,[c] Jianping Yang,[ad] Wei Teng,*[a] Wei-xian Zhang,[a] Guangming Li[a] and Dongyuan Zhao[b]

Received 00th January 2012,
Accepted 00th January 2012

DOI: 10.1039/x0xx00000x

www.rsc.org/MaterialsA

Heterogeneous catalysts showing high catalytic performance, structural stability, and low toxicity, are greatly required for efficiently degenerate organic pollutants in waste water in advanced oxidation processes (AOPs). In this paper, mesoporous heterogeneous catalyst Cu-Mn/TiO_2 composites has been successfully prepared, which has a stable crystalline mesostructure TiO_2 as the support, and well-dispersed Cu-Mn oxides as catalytic active sties. The Cu, Mn content is measured to be 5.7 and 6.0 wt.%, and the BET surface area is measured to be 97 m^2/g with its pore size of ~ 6.0 nm and pore volume of 0.15 cm^3g^{-1}. Using the prepared Cu-Mn/TiO_2 composites as the AOPs catalyst for degeneration of Acid Red 1, it can efficiently (>99%) degenerates the model pollutant in water with only 90 min. Compared with homogeneous catalysts, it can retain its catalytic performance over a wide pH range (3 - 9) and can be recycled for at least five times meanwhile still possessing the decolorization efficiency of 89%. By analyzing the catalytic process, a possible catalytic procedure for degradation of Acid Red 1 has been proposed. Furthermore, using bulk Cu-Mn oxides, Cu-Mn/P25, and Cu-Mn/SBA-15 as reference catalysts, we propose that the excellent catalytic performance of Cu-Mn/TiO_2 could be ascribed to the anatase mesoporous TiO_2, which not only offers a stable matrix with high surface area for Cu-Mn catalysts, but also serves as a kind of catalytic promoter for the synergistic catalytic degeneration of Acid Red 1.

Keywords: mesoporous materials, TiO_2, Cu-Mn oxide, heterogeneous catalysts, advanced oxidation process, water treatment.

Introduction

The contamination of synthetic organic dyes has attracted extensively attention, due to their high toxicity and refractory. Therefore, the treatment of these organics in an economical, effective and energy saving way is of great importance. In this case, advanced oxidation processes (AOPs) might be considered as a priority technology since it can be executed under mild conditions, such as at a low temperature, atmosphere pressure and simply composed of hydrogen peroxide and catalysts [1, 2]. To achieve high efficient degradation of pollutants, catalyst plays a crucial role in AOPs. Although homogeneous catalysts such as Fenton reagent (Fe^{2+}/Fe^{3+}) have been proved to be highly active [3, 4], there still exists some problems, such as unrecyclable, narrow operating condition[5, 6]. To overcome these problems, heterogeneous catalysts have received considerable attention, and various metal oxides have been explored. Among which the Cu and Mn species have shown excellent catalytic performance because of their variable valences as well as wide pH tolerance in water [1, 2, 7-16]. However, to prepare well dispersed Cu and Mn oxides still remains a great challenge.

In this decade, ordered mesoporous materials with interpenetrated and regular mesopore systems have triggered great research interest [17]. They are promising candidates as catalytic supports because of their high surface areas and large pore volumes, which have shown potential application in adsorption and catalysis [18, 19]. As for catalyst supports in AOPs, Li *et al.* synthesized Fe-containing mesoporous carbon materials using soft template routes for degradation of phenol [20]. Melero and co-workers studied the Fe_2O_3/SBA-15 nanocomposite catalyst for treatment of a pharmaceutical wastewater in AOPs [21]. We have also observed that SBA-15 based catalyst show good performance in degradation of Rhodamine B [22]. However, these supports can only serve as a kind of matrix for loading and dispersing the catalysts. A general support, not only having ordered mesostructures but also serving as a potential catalytic promoter, is more required. Mesoporous TiO_2 is an excellent candidate owing to its outstanding features such as environmental friendly, excellent

chemical/thermal stability, as well as excellent electronic and optical properties [23]. Although several efforts have been made to achieve ordered mesoporous TiO_2 [24-26], using mesoporous TiO_2 as catalyst supports for AOPs has been rarely known.

Herein, we report a simple two-step approach to prepare stable ordered mesoporous Cu-Mn/TiO_2 catalyst. It is based on the fabrication of an ultra-stable ordered mesoporous titania by a simple surfactant sulfuric acid carbonization method, and then followed by a post wet-impregnation to get Cu-Mn specise loaded mesoporous TiO_2 and finally calcianted at a settled temeprature. The obtained mesoporous Cu-Mn/TiO_2 catalysts has a surface area of 97 m^2/g, pore size of ~ 6.0 nm. The Cu-Mn oxides are identified to be dispersed well in the mesochannels with the element contents of 5.7 and 6.0 wt.%, respectively. The AOPs catalytic results show that it can efficiently (>99%) degenerate Acid Red 1 in water over a wild range of pH value (3 - 6.7) with only 90 min. Furthermore, a possible catalytic procedure for degradation of Acid Red 1 has been proposed based on the tracking the catalytic reaction.

Experimental

Chemicals

Triblock copolymer Pluronic P123 ($EO_{20}PO_{70}EO_{20}$, with an average molecular weight of M_w = 5800) and titanium isopropoxide [$Ti(OCH(CH_3)_2)_4$, TIPO)] were purchased from Sigma-Aldrich. Ethanol, hydrochloric acid (36.5 wt.%), sulfuric acid (95 - 98 wt.%), copper nitrate tri-hydrate, manganese nitrate solution (50 wt.%), and Acid Red 1 were obtained from Shanghai Chemical Corp. Titanium dioxide P25 was supplied by Degussa Corp. All chemicals were used as received without further purification.

Preparation of catalysts

Ordered mesoporous TiO_2 matrixes were prepared *via* the surfactant sulfuric acid carbonization method according to the report by Zhang *et al* [26], by using titanium isopropoxide (TIPO) as a precursor and amphiphilic triblock copolymer P123 as a template (Scheme 1). A typical synthesis was as follows. 1.0 g of P123 was dissolved in 30 g of ethanol. Then 1.4 g of concentrated HCl and 0.46 g of 44 wt.% H_2SO_4 were added with continuous stirring at 40°C. After 3 h, 3.0 g of TIPO was added with vigorous stirring for 20 h at 40°C. The solution was poured into the dishes to evaporate ethanol at 40°C in air under 50 - 60% relative humidity for about 2 d, and the resultant membranes were dried at 100°C for 2 d. The as-made products were scraped from the dishes. Firstly carbonization was carried out by the residual H_2SO_4 catalyst at 350°C under N_2 atmosphere for 3 h to obtain rigid carbon on the surface of mesochannels. Such resultant product was noted as TiO_2/C. Subsequently, the sample was heated at 450°C in the air atmosphere for 6 h to burn out the carbon and the final pristine mesoporous TiO_2 was obtained.

Cu and Mn species were deposited into mesochannels of the obtained pristine mesoporous TiO_2 by the wet-impregnation (Scheme 1). In a typical preparation, the nitrates precursors containing 0.05 g of copper element and 0.05 g of manganese element were added to a 100 mL beaker containing 1.0 g of support in 50 mL deionized water. The mixture was stirred continuously at 70°C to evaporate the excess water and then dried at 105 °C for 12 h. Afterwards, the resultant samples were calcined at 450 °C for 5 h with a ramping rate of 1°C/min. The final catalysts, mesoporous TiO_2 doped with Cu and Mn species, were obtained and denoted as Cu-Mn/TiO_2. In contrast, the other catalysts, Cu-Mn/P25 and Cu-Mn/SBA-15 were prepared by the same process as that described previously, but using P25 and SBA-15 (which prepared according to Zhao's literature [17]) as supports instead of mesoporous TiO_2, respectively. The L-Cu-Mn/TiO_2 and H-Cu-Mn/TiO_2 were also prepared by the same process, but adding 0.02 g of copper and 0.02 g of manganese element for L-Cu-Mn/TiO_2 and 0.1 g of copper and 0.1 g manganese element for H-Cu-Mn/TiO_2 in nitrates form, respectively. Besides, bulk Cu-Mn oxide without any support was obtained by the evaporation and calcination of the mixed solution of copper nitrate (0.5 mol/L) and manganese nitrate (0.5 mol/L) under the same conditions as the aforementioned process.

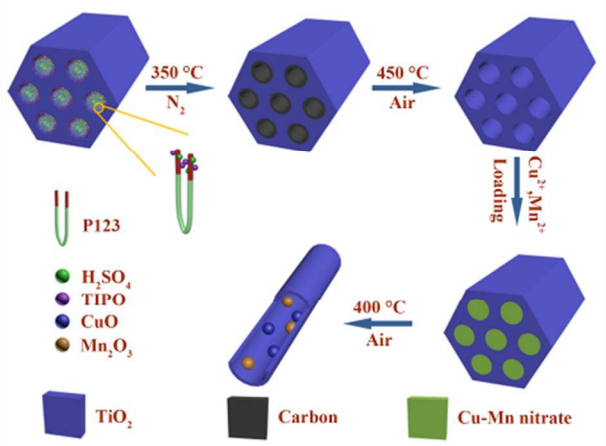

Scheme 1. The preparation of the mesoporous Cu-Mn/TiO_2 composites.

Characterization

Small-angle X-ray scattering (SAXS) measurements were taken on a Nanostar U small-angle X-ray scattering system by using Cu Kα radiation at 40 kV and 35 mA. The *d*-spacing values were calculated by the formula $d = 2\pi/q$, and the unit cell parameters were calculated with the formula $a = 2d_{100}/\sqrt{3}$. Transmission electron microscopy (TEM) images were collected on a JEOL Model 2011 electron microscope operated at 200 kV. Samples were ground in an agate mortar and dispersed in ethanol for 15 min. And the fine suspension was then deposited on a carbon film supported on a molybdenum grid for measurements. Mapping images were also taken by transmission electron microscopy to analyze the distribution of Cu and Mn. Field-emission scanning electron microscopy (FE-SEM) images were obtained with a Hitachi Model S-4800 microscope and the samples without further gold-spraying

treatment were used for observation. N_2 sorption isotherms were measured at 77 K using Micromeritics Model Tristar 3020 analyzer. Prior to the analysis, sample (0.1 g) was degassed under vacuum at 180°C for 6 h. The pore size distribution was derived from the adsorption branches of isotherms using the Barrett-Joyner-Halenda (BJH) model. The pore volume was estimated from the adsorbed amount at p/p_0 of 0.995. The surface area was calculated based on the Brunauer-Emment-Teller (BET) method. X-ray diffraction patterns (XRD) have been recorded on a Bruker D8 Advance diffractometer using Cu Kα radiation source. X-ray photoelectron spectroscopy (XPS) was measured by a Perkin Elmer PHI5000C spectroscope with a Mg Kα line as the excitation source. The atomic contents of metarials was measured by inductively coupled plasma-atomic emission spectrometry (ICP-AES) using a Agilent 720ES. The mineralization of Acid Red 1 solution was quantified by measuring Total organic carbon (TOC) on a Shimadzu 5000A analyzer. The intermediates produced during the degradation of Acid Red 1 in AOPs were identified by Liquid chromatography mass spectrometer (LC–MS) using a Thermo Fisher Scientific TSQ Quantum.

Catalytic activity

Advanced oxidation process reaction was carried out in a glass reactor with 30 mL of Acid Red 1 aqueous solution, and equipped with magnetic stirring and thermostatic bath. After stabilization of temperature, catalysts were added followed by H_2O_2 solution (30 wt.%) to the reactor, this being considered the initial instant of reaction. The whole reaction ran at atmospheric pressure with a constant temperature. In a typical test, 30 mL of the Acid Red 1 solution (200 mg/L), 0.6 g/L of catalyst dosage, and 126.4 mM of H_2O_2 were mixed for the reaction at 70°C and pH 6.7 for 150 min. Periodically, 1 mL of the mixed solution was extracted from the reactor and filtered for further analysis. The residual concentration of Acid Red 1 solution after degraded reaction was measured using a spectrophotometer (Unico SQ2802 UV/VIS) at 530 nm. The decolorization efficiency was used to describe the catalytic degradation of Acid Red 1, which was calculated by the following equation:

$$\text{Decolorization efficiency} = \frac{C_0 - C_t}{C_0} \times 100\% \quad (1)$$

Where, C_0 is the initial concentration, C_t is the concentration at time t.

Pseudo-first order reactions were used to describe the degradation of pollutants by AOPs for kinetic studies. The mass balance in a batch reactor yields:

$$V\frac{dC}{dt} = -(-r)W \quad (2)$$

Where C is the concentration of the Acid Red 1 at instant t, (-r) is the reaction rate, W stands for the mass of catalysts and V is the reaction volume. For a pseudo-first order kinetics (-r = kC), integration of Eq.(2) provides the theoretical history profiles:

$$\frac{C}{C_0} = \exp\left[-k\left(\frac{W}{V}\right)t\right] \quad (3)$$

Where the k is the pseudo first-order kinetic constant and the term (W/V) denotes the catalyst dosage employed, referred here as $C_{catalyst}$.

To evaluate the effects of experimental conditions on degradation reaction, a series of oxidation experiments were carried out under different initial pH values (3 - 9), catalyst dosage (0.0 - 1.0 g/L), initial concentration of H_2O_2 (0.0 - 315.9 mM) and reaction temperature (30 - 90°C). For the reusability of the catalyst, the recycled catalysts were dried at 105°C for 12 h and calcined at 450°C for 5 h before reuse.

Structure, Property and Composition of Cu-Mn/TiO_2

SAXS patterns (Fig. 1Aa) of the pristine mesoporous TiO_2 sample show one obvious scattering peak, suggesting an ordered mesostructure. By loading Cu and Mn species into the mesochannels of the pristine TiO_2, the obtained mesoporous Cu-Mn/TiO_2 composites (Fig. 1Ab) shows less-resolved SAXS pattern with a little right-shift, a sign of inferior mesostructural regularity. The change is partially ascribed to the formation of Cu and Mn nanoparticles, which can absorb X-rays and reduce the contrast between walls and pore voids.

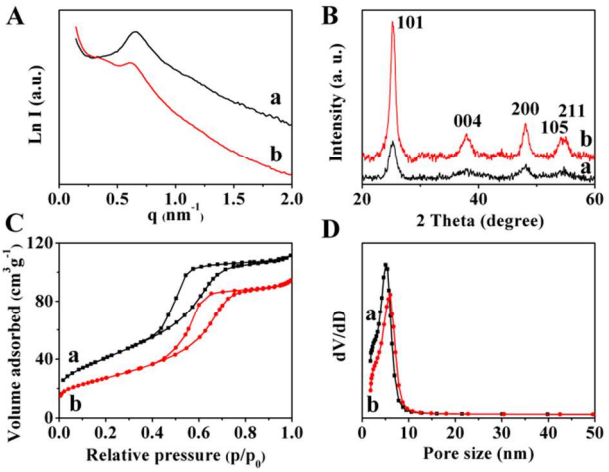

Fig. 1. SAXS patterns (A), wide-angle XRD patterns (B), N_2 adsorption-desorption isotherms (C) and pore size distributions (D) of (a) pristine mesoporous TiO_2 calcined at 450°C for 6 h in air to remove carbon and (b) mesoporous Cu-Mn/TiO_2 composites with metal oxide nanoparticle incorporation *via* post wet-impregnation and calcination at 450°C for 5 h.

Table 1. Structural and textural properties of the samples TiO_2, Cu-Mn/TiO_2, Cu-Mn/SBA-15, Cu-Mn/P25 and bulk Cu-Mn oxide.

Sample	a_0[a] (nm)	Pore size[b] (nm)	V_t (cm^3g^{-1})	S_{BET} (m^2g^{-1})
TiO2	11.1	5.1	0.17	149
Cu-Mn/TiO2	11.9	6.0	0.15	97
Cu-Mn/SBA-15	-	7.1	0.71	412
Cu-Mn/P25	-	-	-	6
Bulk Cu-Mn oxide	-	-	-	25

[a] Cell parameters calculated from SAXS patterns. [b] BET specific surface area evaluated in p/p_0 from 0.02 to 0.20.

Scanning electron microscope (SEM) image (Fig. 2A) of the mesoporous TiO_2 clearly shows open and regularly arranged cylindrical mesopores in a large domain. When the metal oxides are loaded into the mesochannels of the pristine TiO_2, the structural regularity of mesoporous Cu-Mn/TiO_2 composites decreases (Fig. 2B). Furthermore, the opened mesopores on the surface are expaned in a certain degree.

Transmission electron microscope (TEM) image (Fig. 2C) of the mesoporous TiO_2 shows stripe-like patterns in large domains, further confirming a 2D hexagonal mesostructure. After the metal oxides are loaded into the mesochannels of the pristine TiO_2, the ordered mesostructure can be observed (Fig. 2D) in the mesoporous Cu-Mn/TiO_2 composites. High-resolution TEM (HRTEM) images (Fig. 2D inset) manifest that the TiO_2 frameworks are crystallized with the lattices in a *d*-spacing of 0.581 and 0.352, well-matched to the 200 and 101 reflections. Meanwhile, the lattice fringes assigned to Cu and Mn elements can be observed as a result of the homogeneous dispersione of the metal elements. The corresponding elemental mapping (Fig. 3) presents evidence of a homogeneous dispersion of Cu and Mn species on the mesoporous Cu-Mn/TiO_2 composites.

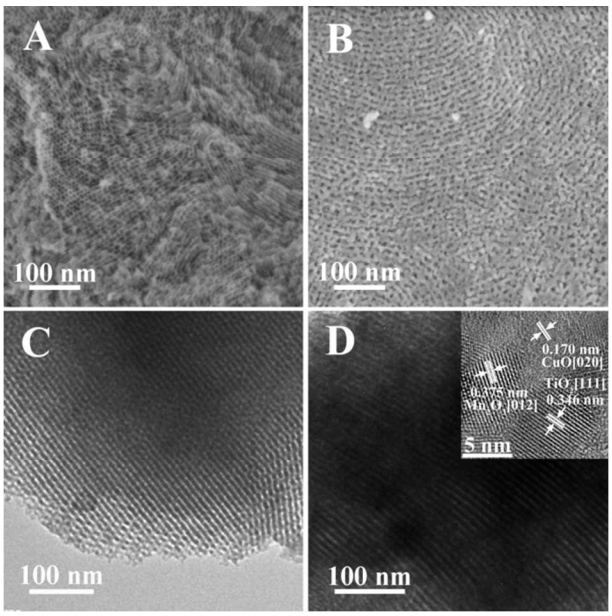

Fig. 2. SEM (A, B), TEM (C, D) and HRTEM (inset in D) images of (A, C) the pristine mesoporous TiO_2 calcined at 450°C for 6 h in air to remove carbon and (B, D) mesoporous Cu-Mn/TiO_2 composites with metal oxide nanoparticle incorporation *via* wet-impregnation and calcination at 450°C for 5 h.

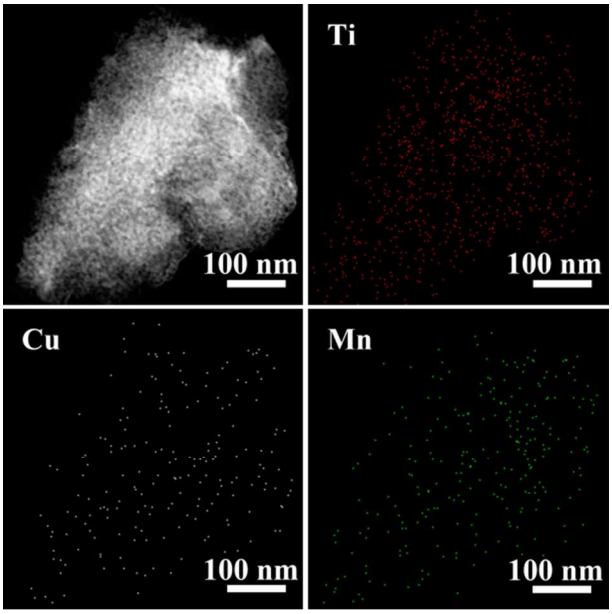

Fig. 3. The STEM image and the corresponding Ti, Cu, and Mn elemental maps of the mesoporous Cu-Mn/TiO_2 composites obtained through the two-step process *via* sulfuric acid carbonization and wet-impregnation.

Nitrogen adsorption-desorption isotherms of the pristine mesoporous TiO_2 before and after the metal oxides loading show representative type-IV curves with H_1 hysteresis loops (Fig. 1C), suggesting a uniform cylindrical mesopore structure. The surface area of pristine mesoporous TiO_2 sample prepared by the surfactanat sulfuric acid carbonization method is high (149 m^2/g), considering the large density of crystalline titania (4.2 g/cm^3). Its pore size is as large as ~ 5.1 nm. After loading of Cu and Mn oxides nanoparticles, the surface area and pore volume of sample Cu-Mn/TiO_2 are decreased to 97 m^2/g and 0.15 cm^3/g, which suggests a successful incorporation of nanoparticles into the mesochannels of TiO_2 matrixes. Interestingly, it is found that the pore size increases from 5.1 to 6.0 nm, in accordance with the results of SAXS and SEM. This can be explained that the precursors of metal oxides may not only access to mesochannels but also into the interspaces between TiO_2 grains. When the metal oxides generate and grow at high calcination temperature, the oxides formed between TiO_2 grains tend to expand the primary interspaces, and finally results in a larger pore size.

The wide-angle X-ray diffraction (XRD) pattern of pure mesoporous TiO_2 reveals four resolved diffraction peaks around 2θ of 25.3, 37.8, 48.1, 53.9 and 55.1 (Fig. 1Ba), which can be assigned to the 101, 004, 200, 105 and 211 reflections of TiO_2 in anatase phase (JCPDS, 21-1272). After Cu and Mn species are loaded into the mesochannels of the pristine TiO_2, the diffraction intensity enhances for the mesoporous Cu-Mn/TiO_2 composites (Fig. 1Bb) at the same position as TiO_2, suggesting a growth in TiO_2 crystallinity. No well-resolved diffraction peaks of Cu or Mn species can be distinguished, which may be attributed to the homogeneous dispersion and low loads of the metal elements on TiO_2.

The mesoporous Cu-Mn/TiO_2 composites was further analyzed using XPS spectra to identify chemical states of Cu, Mn, and Ti species (Fig. 4). Two main peaks of TiO_2 due to Ti $2p_{3/2}$ and Ti $2p_{1/2}$ are observed at 458.4 and 464.1 eV, respectively. Peak of Cu $2p_{3/2}$ at 933.6 eV indicates that Cu mainly exists in the form of Cu (II) [27, 28]. The binding energy peak of Mn $2p_{3/2}$ at 641.4 eV can be assigned to Mn (III) [29-31]. Furthermore, the contents of different elements (Ti, Cu and Mn) are 50.6, 5.7 and 6% (Table S1), which are detected by inductively coupled plasma-atomic emission spectrometry (ICP-AES).

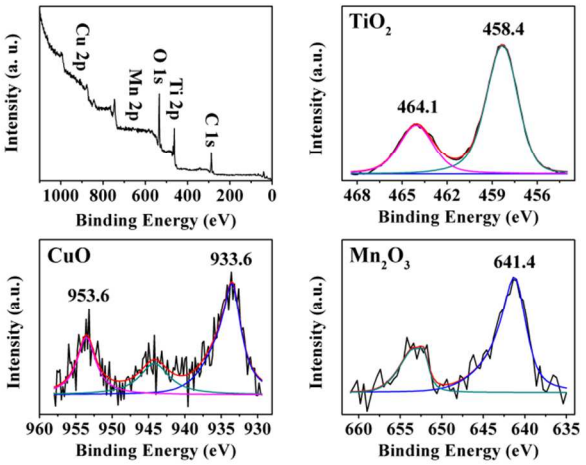

Fig. 4. XPS spectra of the mesoporous Cu-Mn/TiO_2 composites obtained through the two-step process *via* sulfuric acid carbonization and wet-impregnation.

Catalytic performance

The catalytic performances of the pristine mesoporous TiO_2, Cu-Mn/TiO_2 composites, pure P25, bulk Cu-Mn oxide and other supported Cu-Mn composites (Cu-Mn/P25, Cu-Mn/SBA-15) were investigated by adopting Acid Red 1 (200 mg/L) as a model pollutant (Fig. 5). The reaction conditions used in the comparison experiment are 6.7 of initial pH value, 1.0 mg/L of catalyst dosage, 126.4 mM of H_2O_2 concentration and 70°C. Firstly, for comparison, no catalysts but only H_2O_2 is used. 4% of degradation efficiency suggests that solid catalyst plays a key role for the degradation of Acid Red 1. Then, the bulk Cu-Mn oxide without supports presents 29% of degradation efficiency, while the supported Cu-Mn oxide catalysts Cu-Mn/P25 and Cu-Mn/SBA-15 show 33 and 65% respectively, confirming the significant effect of a support. Among all the catalysts, the mesoporous Cu-Mn/TiO_2 composites shows the highest activity for the degradation of Acid Red 1, its decolorization efficiency can reach 99% within 150 min at 70°C. Moreover, the pristine mesoporous TiO_2 catalyst and P25 without Cu-Mn oxide loading exhibit 86% and 8% of degradation efficiency at the same reaction conditions, respectively. The mobile hydroxyl radicals are generated on anatase TiO_2 but not on rutile [32]. Therefore, 20% of TiO_2 in P25 exists in the form of rutile phase, which may be one of the causes for the low degradation efficiency. Whereas, the outstanding catalytic performance of the pristine mesoporous TiO_2 mainly due to its mesostructure. The opened mesopore of Cu-Mn/TiO_2 composite contributes to transition of large molecules and provides enough space for adsorption and reaction. When no H_2O_2 is added, the pristine mesoporous TiO_2 only shows 2% of degradation efficiency, suggesting that adsorption effect contributes little to the decolorization at pH 6.7.

The effect of Cu and Mn loads on the activity of catalysts in the degradation of Acid Red 1 is investigated. The catalyst containing 5.7 wt.% of Cu and 6.0 wt.% of Mn shows the best performance (99%) for Acid Red 1 removal (Table S1). Therefore, the best Cu-Mn/TiO_2 composite is taken as typical catalyst for forenamed discussion. The mesoporous Cu-Mn/TiO_2 composites is stable and can be reused for several times. It maintains high decolorization efficiency of 89% after five consecutive recycles (Fig. S1). Meanwhile, the performance of the sample Cu-Mn/TiO_2 for the degradation of Acid Red 1 was studied in a wide range of pH value from 3 to 9. It is found that the catalytic performance is high to 99%, as varying the initial pH of the dye solution between 3 and 6.7 (Fig. S2A). Although decolorization rate decreases as increasing pH from 6.7 to 9, it must be stressed that the decolorization efficiency still can reach 90% when the reaction is operated at pH 9 for 150 min. This is an important advantage because it allows efficient degradation of Acid Red 1 in a large range of pH, which is very meaningful for wastewater treatment in practice. The optimized reaction conditions are obtained by a series of investigation into the effects of external factors, that 0.8 mg/L of catalyst dosage, 126.4 mM of H_2O_2 and 70°C for reaction are benefit for the catalytic performance (Fig. S2). More remarkable, the reaction equilibrium time is very short with only 5 min. The exponential relationship between (C/C_0) and reaction time (t) with good correlation coefficient ($R^2 > 0.99$), indicating that the degradation reaction follows the pseudo-first order kinetic model (Fig. S3). The dependence of the kinetic constant on the reaction temperature (Fig. S4) evidences an Arrhenius behavior, with an activation energy of 75.7 kJ/mol.

Considering the performance of the catalysts with different components and structures, it can be inferred that several significant factors lead to such results for the oxidation of Acid Red 1. First of all, a catalyst can trigger more efficient active sites. The generation of hydroxyl radical is regarded as a paramount active part to efficiently mineralize pollutants in AOPs. H_2O_2 treatment without the application of an active catalyst is not feasible for the degradation (only 4%) of pollutants because only few hydroxyl radicals can be triggered to generate. Secondly, proper support with unique feature is crucial to enhance the catalytic performance for AOPs. The bulk Cu-Mn oxides with a small surface area (25 m^2/g) shows lowest degradation efficiency in the presence of catalysts, because of the serious aggregation (Fig. S5) to largely reduce the accessible active sites without the support for location and separation. On the other hand, the mesoporous solids as a support, such as mesoporous silica SBA-15 and titanium dioxide, exhibit higher catalytic performance than that with

nonporous P25. It can be explained that the mesoporous materials possess a high surface area, a large pore volume and interconnected mesopore channels, which can not only offer enormous sites to locate and disperse the metallic oxides nanoparticles but also as a confined space to hinder their further growth and aggregation (Fig. S6). In addition, such advantages of its special structure facilitate fast molecular diffusion and transportation for pollutants to contact the active sites in inner mesopore channels. Thirdly, the natural activity of supports is another key for catalytic performance. Titania is a promising potential support for metal oxieds catalysts due to its outstanding electronic and optical properties. When SBA-15 is used as a support (Fig. S7), in spite of its unique mesostructure and even higher porosity than mesoporous TiO_2, its intrinsic nature of silica frameworks cannot supply any assistants for oxidation [22]. Therefore, utilization of mesoporous TiO_2 as a support combines both merits of its special framework component and mesopore structure for further improvement of degradation efficiency. Consequently, the highest catalytic efficiency for Cu-Mn/TiO_2 nanocomposites can be contributed to a synergetic interaction regime, including the synergic effects of Cu-Mn oxides and TiO_2 components, and unique structure with confined and interconnected mesochannels for supporting metallic oxides nanoparticles and molecules transportation.

In addition, the leaching experiment shows that after solid catalyst is removed by centrifugation at 5 min, only 67% of the final decolorization efficiency at 150 min is obtained. With the same reaction conditions, the decolorization efficiency can reach 64 and 99% at 5 and 40 min, respectively, suggesting that this is a heterogeneous catalytic reaction.

In degradation of Acid Red 1, hydroxyl radicals as main oxidant can attack and break the azo group (–N=N–) of the molecule, which is responsible for decolorization. The results of Total organic carbon (TOC) test for the final solution show that 68% of Acid Red 1 is mineralized completely. Liquid chromatography mass spectrometer (LC–MS) experiment is executed to identify the formation of intermediates during the degradation process. The results (Table S2) show that several naphthalenic and benzenic derivatives were detected. Based on the intermediates analyzed by LC–MS, a probable degradation mechanism is proposed. Fig S9 presents the proposed reaction pathway for degradation of Acid Red 1 by the AOPs.

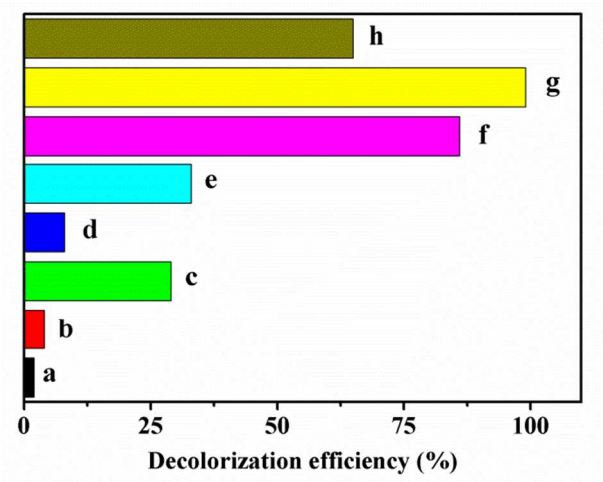

Fig. 5. Catalytic performance on the degradation of Acid Red 1 by using (a) 1.0 g/L of the pristine mesoporous TiO_2 without H_2O_2 addition, (b) no catalyst, (c) 1.0 g/L of bulk Cu-Mn oxide, (d) 1.0 g/L of P25, (e) 1.0 g/L of Cu-Mn/P25, (f) 1.0 g/L of the pristine mesoporous TiO_2, (g) 1.0 g/L of the mesoprous Cu-Mn/TiO_2 composites, and (h) 1.0 g/L of mesoporous Cu-Mn/SBA-15 ($C_{H_2O_2}$ = 126.4 mM, T = 70°C, pH = 6.7).

Conclusions

In summary, novel mesoporous Cu-Mn/TiO_2 catalysts have been successfully prepared by a two-step approach. The ordered mesoporous composites has a high surface area (97 m^2/g), uniform pore size (~ 6.0 nm), large pore volume (0.15 cm^3/g) and well crystalline frameworks. The catalyst Cu-Mn oxides nanoparticles are well introduced into the mesochannels with the contents of 5.7 and 6.0 wt.%. The catalytic results confirmed that it has high catalytic perfomance (99%) and a wide range of pH (3 - 9) for degeneration of Acid Red 1 in AOPs, and can be recycled at least five times. Based on the comparasion studies, we propose that the excellent catalytic performance of Cu-Mn/TiO_2 could be ascribed the anatase mesoporous TiO_2, which not only offers a stable matrix with high surface area for Cu-Mn catalysts, but also serves as a kind of catalytic promoter for the synergistic catalytic degeneration of Acid Red 1.

Acknowledgements

We acknowledge supports from the State Key Laboratory of Pollution Control and Resource Reuse Foundation (PCRRF12001), Shanghai Scientific Research Plan Project (14R21411300), China Postdoctoral Science Foundation (2014M551455), China Postdoctoral Science Foundation (2014M561520), the Economic and Information Committee Cooperation Plan of Shanghai (04002530571), and the Science and Technology Committee Plan of Shanghai Qingpu District (04002370168).

Notes and references

[a] College of Environmental Science and Engineering, State Key Laboratory of Pollution Control and Resource Reuse, Tongji University, No. 1239, Siping Road, Shanghai 200092, P. R. China.
[b] Department of Chemistry, Laboratory of Advanced Materials, Fudan University, Shanghai 200433, P. R. China.
[c] Shanghai Tongji Clearon Environmental-Protection Equipment Engineering Co., Ltd, Shanghai 200092, P. R. China.
[d] Institute for Superconducting & Electronic Materials, Australian Institute of Innovative Materials, University of Wollongong, Innovation Campus, Squires Way, North Wollongong, NSW 2500, Australia.
*E-mail address: fanjianwei@tongji.edu.cn (Dr. Jianwei Fan)
wteng@tongji.edu.cn (Dr. Wei Teng)
Tel: +86-21-65982658
Fax: +86-21-65985157
‡ These authors contributed equally to this work.
Electronic Supplementary Information (ESI) available: [details of any supplementary information available should be included here]. See DOI: 10.1039/b000000x/

1 N. Inchaurrondo, J. Cechini, J. Font and P. Haure, *Appl. Catal. B-Environ.*, 2012, **111**, 641-648.
2 J. Barrault, C. Bouchoule, K. Echachoui, N. Frini-Srasra, M. Trabelsi and F. Bergaya, *Appl. Catal. B-Environ.*, 1998, **15**, 269-274.
3 H. J. H. Fenton, *Journal of the Chemical Society*, 1894, **65**, 899-910.
4 C. Walling, *Acc. Chem. Res.*, 1975, **8**, 125-131.
5 M. Hartmann, S. Kullmann and H. Keller, *J. Mater. Chem.*, 2010, **20**, 9002-9017.
6 Y. H. Zhan, X. A. Zhou, B. Fu and Y. L. Chen, *J. Hazard. Mater.*, 2011, **187**, 348-354.
7 S. X. Yang, Z. Q. Liu, X. H. Huang and B. P. Zhang, *J. Hazard. Mater.*, 2010, **178**, 786-791.
8 P. Massa, M. A. Ayude, F. Ivorra, R. Fenoglio and P. Haure, *Catal. Today*, 2005, **107-08**, 630-636.
9 R. Levi, M. Milman, M. V. Landau, A. Brenner and M. Herskowitz, *Environ. Sci. Technol.*, 2008, **42**, 5165-5170.
10 S. C. Kim and D. K. Lee, *Catal. Today*, 2004, **97**, 153-158.
11 H. T. Gomes, P. Selvam, S. E. Dapurkar, J. L. Figueiredo and J. L. Faria, *Micropor. Mesopor. Mater.*, 2005, **86**, 287-294.
12 H. Chen, A. Sayari, A. Adnot and F. Larachi, *Appl. Catal. B-Environ.*, 2001, **32**, 195-204.
13 F. Arena, R. Giovenco, T. Torre, A. Venuto and A. Parmaliana, *Appl. Catal. B-Environ.*, 2003, **45**, 51-62.
14 A. Alejandre, F. Medina, X. Rodriguez, P. Salagre, Y. Cesteros and J. E. Sueiras, *Appl. Catal. B-Environ.*, 2001, **30**, 195-207.
15 M. Abecassis-Wolfovich, M. V. Landau, A. Brenner and M. Herskowitz, *J. Catal.*, 2007, **247**, 201-213.
16 R. J. G. Lopes, M. L. N. Perdigoto and R. M. Quinta-Ferreira, *Appl. Catal. B-Environ.*, 2012, **117**, 292-301.
17 D. Y. Zhao, J. L. Feng, Q. S. Huo, N. Melosh, G. H. Fredrickson, B. F. Chmelka and G. D. Stucky, *Science*, 1998, **279**, 548-552.
18 J. Liu, S. Z. Qiao, Q. H. Hu and G. Q. Lu, *Small*, 2011, **7**, 425-443.
19 W. Teng, Z. Wu, J. Fan, H. Chen, D. Feng, Y. Lv, J. Wang, A. M. Asiri and D. Zhao, *Energ Environ Sci*, 2013, **6**, 2765.
20 J. S. Li, J. Gu, H. J. Li, Y. Liang, Y. X. Hao, X. Y. Sun and L. J. Wang, *Micropor. Mesopor. Mater.*, 2010, **128**, 144-149.
21 J. A. Melero, F. Martinez, J. A. Botas, R. Molina and M. I. Pariente, *Water Res.*, 2009, **43**, 4010-4018.
22 J. Fan, X. Jiang, H. Min, D. Li, X. Ran, L. Zou, Y. Sun, W. Li, J. Yang, W. Teng, G. Li and D. Zhao, *Journal of Materials Chemistry A*, 2014, **2**, 10654-10661.
23 P. Doggali, Y. Teraoka, P. Mungse, I. K. Shah, S. Rayalu and N. Labhsetwar, *J. Mol. Catal. A: Chem.*, 2012, **358**, 23-30.
24 J. Fan, Y. Dai, Y. Li, N. Zheng, J. Guo, X. Yan and G. D. Stucky, *J. Am. Chem. Soc.*, 2009, **131**, 15568-155689.
25 P. D. Yang, D. Y. Zhao, D. I. Margolese, B. F. Chmelka and G. D. Stucky, *Chem. Mater.*, 1999, **11**, 2813-2826.
26 R. Y. Zhang, B. Tu and D. Y. Zhao, *Chem-Eur J*, 2010, **16**, 9977-9981.
27 L. H. Zhang, F. Li, D. G. Evans and X. Duan, *Ind. Eng. Chem. Res.*, 2010, **49**, 5959-5968.
28 C. D. Wagner, W. M. Riggs, L. E. Davis, J. F. Moulder and G. E. Muilenberg, *Handbook of X-Ray Photoelectron Spectroscopy*, Perkin-Elmer Corporation, Eden Prairie, Minnesota, 1979.
29 M. Ferrandon, J. Carno, S. Jaras and E. Bjornbom, *Appl Catal a-Gen*, 1999, **180**, 141-151.
30 M. R. Morales, B. P. Barbero and L. E. Cadus, *Appl. Catal. B-Environ.*, 2006, **67**, 229-236.
31 Y. J. Kim, H. J. Kwon, I. Heo, I.-S. Nam, B. K. Cho, J. W. Choung, M.-S. Cha and G. K. Yeo, *Applied Catalysis B: Environmental*, 2012, **126**, 9-21.
32 W. Kim, T. Tachikawa, G. H. Moon, T. Majima and W. Choi, *Angew. Chem. Int. Edit.*, 2014, **53**, 14036-14041.

Graphical Abstract

Preparation of mesoporous Cu-Mn/TiO_2 composites for degradation of Acid Red 1

Hongyang Min,‡[a] Xianqiang Ran,‡[a] Jianwei Fan,*[ab] Yu Sun,[c] Jianping Yang,[ad] Wei Teng,*[a] Wei-xian Zhang,[a] Guangming Li[a] and Dongyuan Zhao[b]

A simple two-step method was adopted to prepare the mesoporous Cu-Mn/TiO_2 composites, which shows high catalytic activity for degradation of Acid Red 1.